Article

Syntheses of Highly Fluorescent GFP-Chromophore Analogues

Liangxing Wu, and Kevin Burgess

J. Am. Chem. Soc., **2008**, 130 (12), 4089-4096• DOI: 10.1021/ja710388h • Publication Date (Web): 06 March 2008

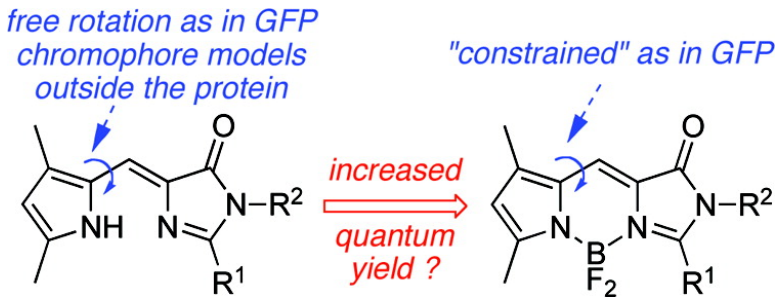

More About This Article

Additional resources and features associated with this article are available within the HTML version:

- Supporting Information
- Links to the 1 articles that cite this article, as of the time of this article download
- Access to high resolution figures
- Links to articles and content related to this article
- Copyright permission to reproduce figures and/or text from this article

View the Full Text HTML

J|A|C|S
ARTICLES
Published on Web 03/06/2008

Syntheses of Highly Fluorescent GFP-Chromophore Analogues

Liangxing Wu and Kevin Burgess*

Department of Chemistry, Texas A & M University, Box 30012, College Station, Texas 77841

Received December 4, 2007; E-mail: burgess@tamu.edu

Abstract: Eight B-containing compounds, i.e., **1a**−**h**, were prepared as mimics of the green fluorescent protein (GFP) fluorophore. The underlying concept was that synthetic GFP chromophore analogues are not fluorescent primarily because of free rotation about an aryl−alkene bond (Figure 1b). This rotation is not possible in the β-barrel of GFP; hence, the molecule is strongly fluorescent. In compounds **1a**−**h**, radiationless decay via this mechanism is prevented by complexation of the BF_2 entity. The target materials were prepared via two methods; most were obtained according to the novel route shown in Scheme 1b, but compound **1f** was made via the procedure described in Scheme 2. Both syntheses involved formation of undesired compounds *E*-**4a**−**h** that formed simultaneously with the desired isomeric intermediates *Z*-**4a**−**h**. Both compounds form BF_2 adducts, i.e., **1a**−**h** and **5a**−**h**, respectively. Methods used for spectroscopic characterization and differentiation of compounds in the series **1** and **5** are discussed, and these are supported by single-crystal X-ray diffraction analyses for compounds **1c**, **5c**, **1f**, and **5f**. Electronic spectra of compounds **1a**−**h** and **5a**−**h** were studied in detail. Those in the **5** series were shown to be only weakly fluorescent, but the **1** series were strongly fluorescent compounds (comparable to the boraindacene, BODIPY, dyes). Compounds **1g** and **1h** are water soluble, and **1h** has particularly significant potential as a probe, since it also has a carboxylic acid group for attachment to biomolecules.

Introduction

Expression of proteins attached to green fluorescent protein (GFP; Figure 1a) is one of the most widely used strategies for labeling inside live cells.[1−5] Most of the GFP molecule is not directly useful for the fluoresence of this material; in fact, the chromophore is relatively small (Figure 1b).[6,7] The GFP chromophore is formed via autocatalytic dehydration of a Ser-Tyr-Gly tripeptide motif to give an imidazolinone that is then air-oxidized (Figure 1c).[8] Chromophores in GFP analogues are formed via similar condensation/oxidation routes from other tripeptides (e.g., blue fluorescent protein, BFP, from Ser-His-Gly; cyan fluorescent protein, CFP, from Ser-Trp-Gly).[1,8]

Molecules representing the chromophores of GFP (**A**[9] and **B**[6]) and point mutants (**C** for Y66F mutant of GFP; **D** for cyan fluorescent protein CFP representing the Y66W mutant of GFP; **E** for blue fluorescent protein BFP representing the Y66H mutant of GFP)[9] or naturally occurring analogues (**F** for red fluorescent protein RFP)[10] have been prepared and studied in solution.[11,12] They fluoresce at somewhat shorter wavelengths than their parent proteins and *with extremely low quantum yields.* This striking difference in quantum yields has been much discussed in the literature, but the consensus opinion is relatively simple.[13] Loss of fluorescence energy from the synthetic chromophores in solution is mainly the result of radiationless transfer arising from free rotation about the aryl−alkene bond (blue arrows, Figure 2). Isomerization of the alkene (red arrows) and the polar nature of aqueous media relative to the apolar environment within the β-barrel protein structures may also be contributing factors, but the main one is that free rotation parameter. Steric and electronic factors prevent free rotation of the aryl substituents when the chromophores are encapsulated in the proteins. The environment also disfavors *E*/*Z*-isomerization and provides an apolar medium that is often conducive to fluorescence.

The research discussed here explores a hypothesis that highly fluorescent analogues of the GFP chromophore could be made by including boron. The conceptual genesis of these analogues **1** and the particular compounds that in fact have now been made are represented in Figure 3. It was supposed that inclusion of the boron atom would preclude free rotation of the aryl−alkene bond, so these chromophore analogues would be highly fluorescent in solution. Further, the structures of the target

(1) Tsien, R. Y. *Annu. Rev. Biochem.* **1998**, *67*, 509−544.
(2) Tsien, R. Y. *Annu. Rev. Neurosci.* **1989**, *12*, 227−253.
(3) Miller, L. W.; Cai, Y.; Sheetz, M. P.; Cornish, V. W. *Nat. Methods* **2005**, *2*, 255−257.
(4) Wang, S.; Hazelrigg, T. *Nature* **1994**, *369*, 400−403.
(5) Chalfie, M.; Tu, Y.; Euskirchen, G.; Ward, W. W.; Prasher, D. C. *Science* **1994**, *263*, 802−805.
(6) Niwa, H.; Inouye, S.; Hirano, T.; Matsuno, T.; Kojima, S.; Kubota, M.; Ohashi, M.; Tsuji, F. I. *Proc. Natl. Acad. Sci. U.S.A.* **1996**, *93*, 13617−13622.
(7) Shimomura, O. *FEBS Lett.* **1979**, *104*, 220−222.
(8) Zimmer, M. *Chem. Rev.* **2002**, *102*, 759−781.
(9) Kojima, S.; Ohkawa, H.; Hirano, T.; Maki, S.; Niwa, H.; Ohashi, M.; Inouye, S.; Tsuji, F. I. *Tetrahedron Lett.* **1998**, *39*, 5239−5242.
(10) He, X.; Bell, A. F.; Tonge, P. J. *Org. Lett.* **2002**, *4*, 1523−1526.
(11) Dong, J.; Solntsev, K. M.; Poizat, O.; Tolbert, L. M. *J. Am. Chem. Soc.* **2007**, *129*, 10084−10085.
(12) Chen, K.-Y.; Cheng, Y.-M.; Lai, C.-H.; Hsu, C.-C.; Ho, M.-L.; Lee, G.-H.; Chou, P.-T. *J. Am. Chem. Soc.* **2007**, *129*, 4510−4511.
(13) Follenius-Wund, A.; Bourotte, M.; Schmitt, M.; Iyice, F.; Lami, H.; Bourguignon, J.-J.; Haiech, J.; Pigault, C. *Biophys. J.* **2003**, *85*, 1839−1850.

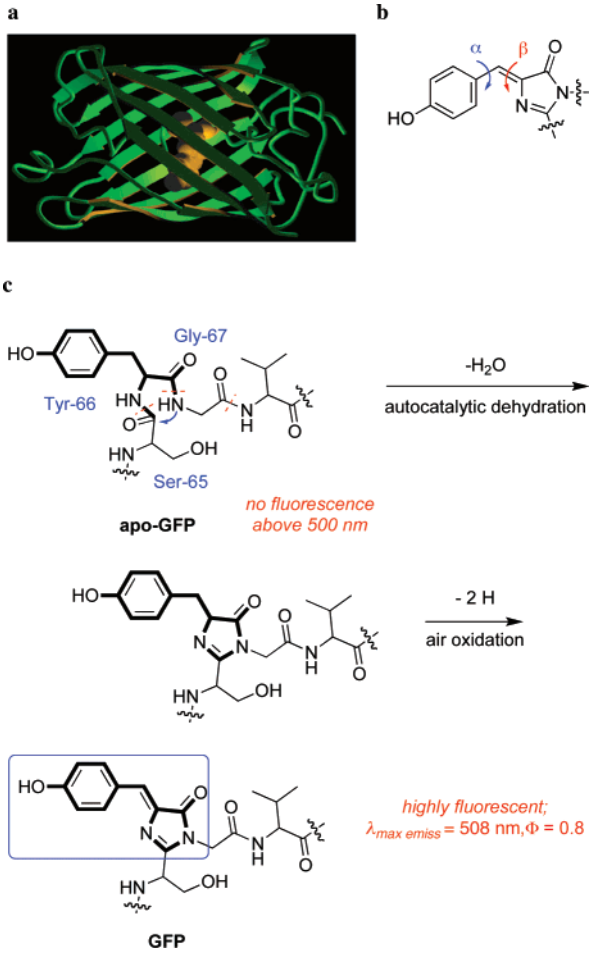

Figure 1. GFP: (a) X-ray structure; (b) chromophore; (c) biogenesis of the chromophore.

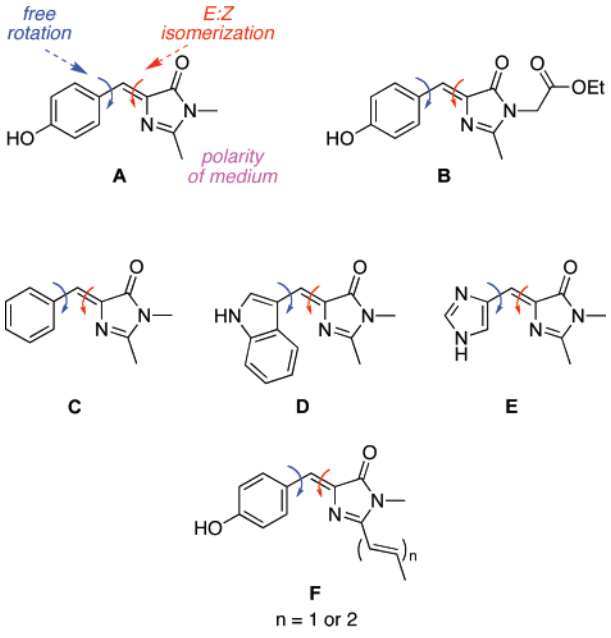

Figure 2. Some synthetic analogues of chromophores in strongly fluorescent proteins.

molecules **1** are reminiscent of the highly fluorescent dyes in the 4,4-difluoro-4-bora-3a,4a-diaza-*s*-indacene, or BODIPY (hereafter abbreviated to BODIPY) class, **G**.[14] Thus, this paper

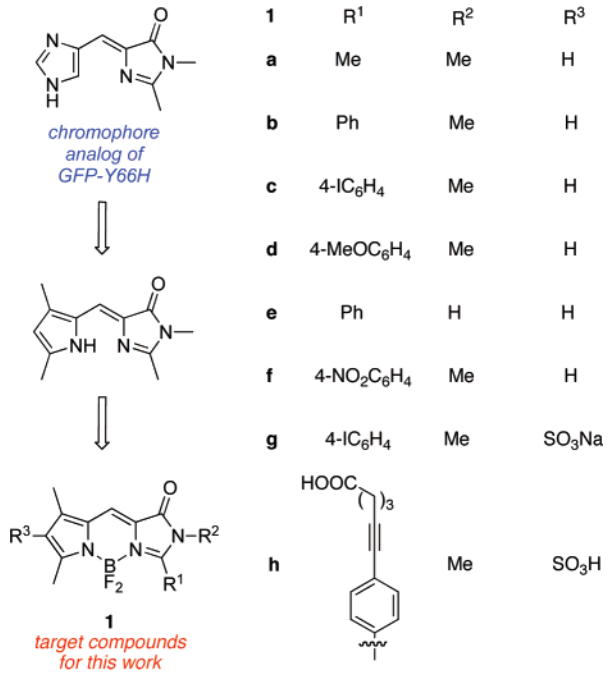

Figure 3. Thought process that led to the design of analogues **1** and the derivatives discussed in this paper.

concerns the syntheses and photophysical properties of compounds **1a**−**h**.

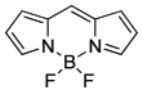

G
BODIPY core

Results and Discussion

Syntheses of the Highly Fluorescent GFP-Chromophore Analogues. To the best of our knowledge, nearly[6] all the syntheses of GFP-chromophore analogues are based on condensation of hippuric or aceturic acid derivatives with aldehydes (the "Erlenmeyer azlactone synthesis"[15]).[9,12,13,16−18] However, at least one report indicates these conditions do not work well for pyrrole-2-carbaldehyde,[19] and in fact, attempts to use them for this substrate were unsuccessful (Scheme 1a). Consequently, a new strategy was developed that began with the synthesis of an imidazolinone and then condensation of this with the pyrrole−aldehyde. That route was successful for compounds **1a**−**e**.

We initially believed the main challenge in the synthesis described in Scheme 1b was that compounds **4** tended to form as mixtures of *E*/*Z* isomers, but later it was determined that these materials isomerized under the reaction conditions to form **1** and **5**. This conclusion was reached in the following way. Compound **1c** and the corresponding intermediates **4c** were chosen as models for the series. First, evidence was collected for assignment of *E*- or *Z*-stereochemistry for **4c** and related

(14) Loudet, A.; Burgess, K. *Chem. Rev.* **2007**, *107*, 4891−4932.
(15) Erlenmeyer, E. *Justus Liebigs Ann. Chem.* **1893**, *275*, 1−8.
(16) He, X.; Bell, A. F.; Tonge, P. J. *FEBS Lett.* **2003**, *549*, 35−38.
(17) Bourotte, M.; Schmitt, M.; Follenius-Wund, A.; Pigault, C.; Haiech, J.; Bourguignon, J.-J. *Tetrahedron Lett.* **2004**, *45*, 6343−6348.
(18) Yampolsky, I. V.; Remington, S. J.; Martynov, V. I.; Potapov, V. K.; Lukyanov, S.; Lukyanov, K. A. *Biochemistry* **2005**, *44*, 5788−5793.
(19) Herz, W. *J. Am. Chem. Soc.* **1949**, *71*, 3982−3984.

Scheme 1. Routes to Target Compounds **1**[a]

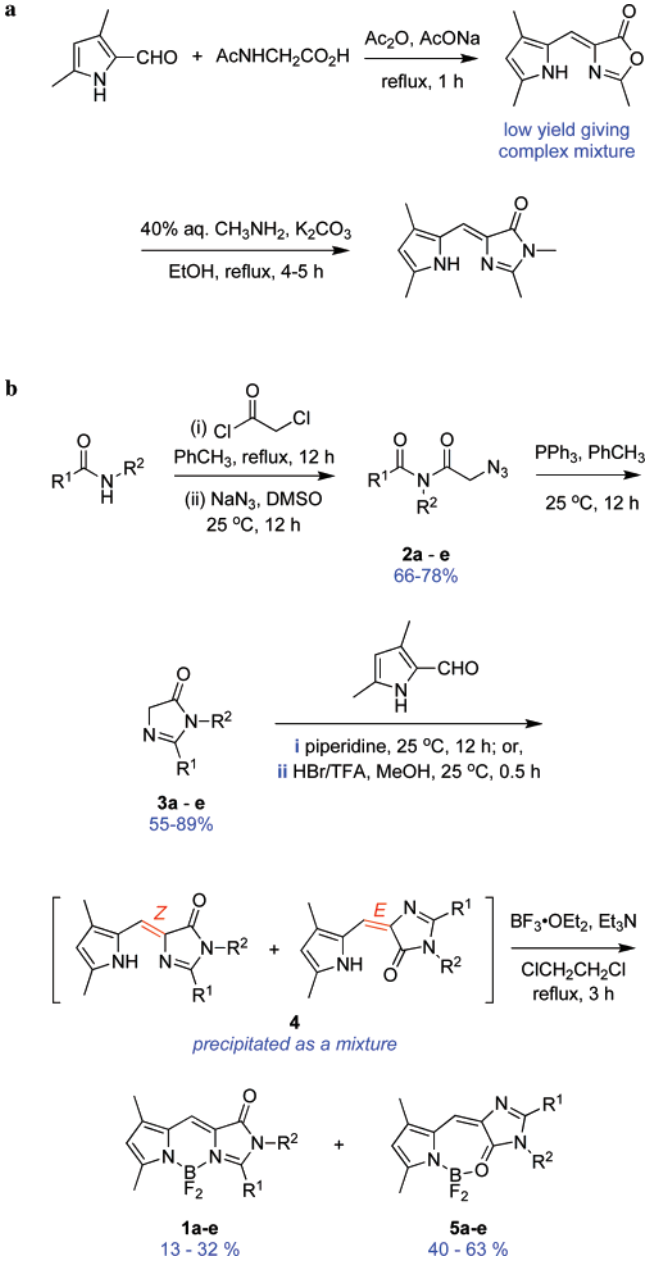

[a] (a) Conventional condensation approaches were unsuccessful for pyrrole-2-carboxaldehyde; (b) the strategy developed here involving condensation of imidazolinones.

materials.[16,20] Table 1 shows selected spectroscopic parameters for the two isomers of **4c**. Coupling between the C^6−*H* proton and the *C*^{5}═O carbonyl carbon was probably the most definitive stereochemical probe; a larger coupling constant was observed for one isomer that was therefore assigned an *E*-configuration. This assignment was supported by observation of a reduced wavenumber for stretching of the carbonyl group in the putative *E*-isomer, as would be expected from internal H-bonding. With this assignment, chemical shift differences of the protons at H^6, H$^{1'}$, H$^{4'}$ and the carbon at C^5 were noted as possible indicators of *E*- or *Z*-stereochemistry.

Work by others on syntheses of GFP-chromophore analogues (via approaches analogous to that shown in Scheme 1a) leading

Table 1. Spectroscopic Properties of *Z*- and *E*-**4c** Isomers

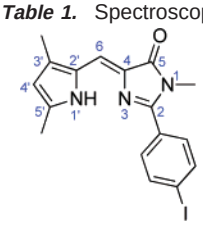

Z-4c

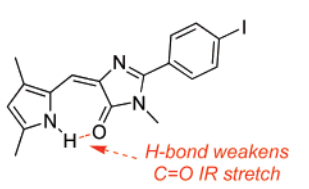

E-4c

	$^3J_{H6,C5}$ (Hz)	$\nu_{C=O}$ (cm^{-1})	δ_{H6} (ppm)	δ_{C5} (ppm)	$\delta_{H1'}$ (ppm)	$\delta_{H4'}$ (ppm)
Z-**4c**	3.8	1686	7.17	169.8	10.62	5.87
E-**4c**	8.9	1663	7.33	168.6	13.01	5.99

to compounds like **H**[9] and **I**[18] could have led to isomeric mixtures, but apparently that was not a problem for those

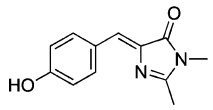

H

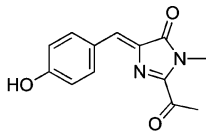

I

structures. Thus, the *Z*-isomer of compound **H** was shown to be more stable than the *E*-form via experimental measurements.[16] Similarly, B3LYP calculations for molecule **I** indicated that the *Z*-isomer was thermodynamically preferred.[21] However, the same B3LYP method was applied to compound **4c** in the current work, and this led to the wrong conclusion. Specifically, the *E*-isomer was calculated to be more stable both *in vacuo* and in a medium of the same dielectric constant as DMSO (by 1.33 and 0.61 kcal·mol^{-1} at 25 °C and by 0.82 and 0.60 kcal·mol^{-1} at 100 °C, respectively), whereas NMR experiments in DMSO-d_6 showed that the *Z*-isomer was in fact the thermodynamically preferred one. Details of the calculations are given in the Supporting Information, and spectra for the thermal isomerization studies are shown in Figure 4a. In fact, the thermal isomerization in DMSO-d_6 at 100 °C was quite slow (the reaction approaches equilibrium after 51 h, indicative of a very high-energy barrier to *E*,*Z* isomerization). The *E*,*Z* ratio at equilibrium was about 0.6:1.0, indicating that the *Z*-isomer was more stable by 0.41 kcal·mol^{-1} at 100 °C. Photoisomerization of two different *E*/*Z* mixtures of **4c** in $CDCl_3$ irradiated at 360 nm was also studied; the data (Figure 4b) indicate that the *E*-isomer is dominant in the photostationary state.

The next step in this project was to make the final products **1** from the intermediates **4**. Two isomeric products could be formed, **1** and **5**, and the spectroscopic strategies used to differentiate them were similar but not identical to those applied to compound **4c**. Coupling between the C^6−*H* proton and the *C*^{5}═O carbonyl carbon is complicated by additional spin pairings involving the B and ^{19}F nuclei. Consequently, that particular spectroscopic probe is not so conveniently measured; however, the *E*-isomer is easily identified by the presence of coupling between the ^{19}F to *C*^{5}═O atoms. Further, the carbonyl stretch for compounds **5** is less than that for **1**; in this case, this is because the boron atom is directly coordinated with the

(20) de Dios, A.; Luz de la Puente, M.; Rivera-Sagredo, A.; Espinosa, J. F. *Can. J. Chem* **2002**, *80*, 1302−1307.

(21) Nemukhin, A. V.; Topol, I. A.; Burt, S. K. *J. Chem. Theory Comput.* **2006**, *2*, 292−299.

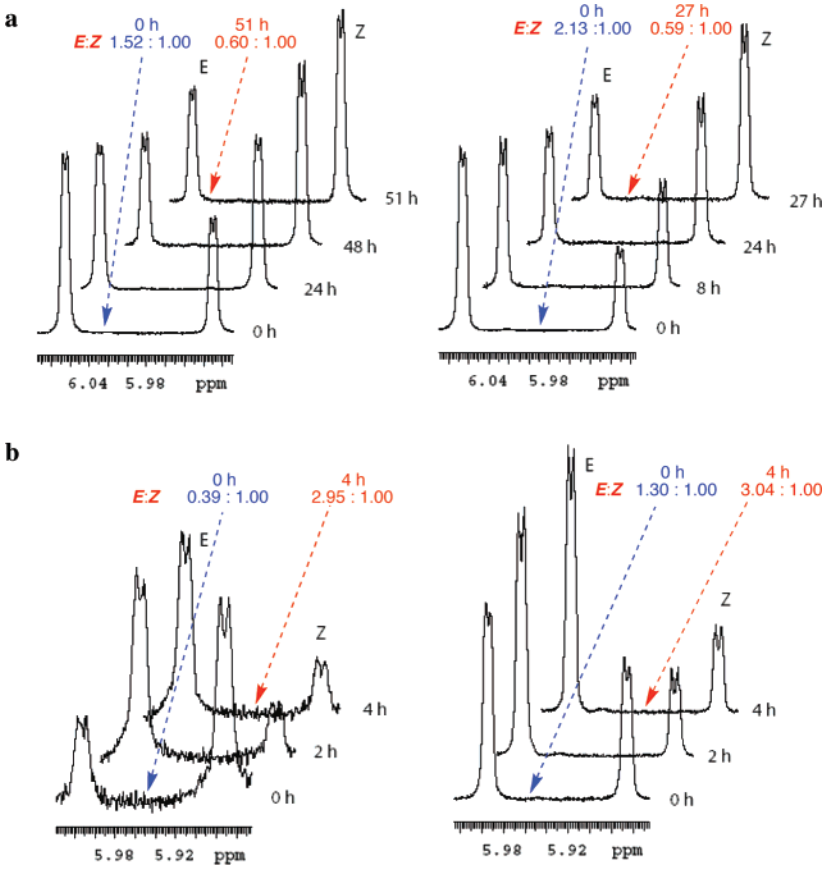

Figure 4. Isomerization of *E*,*Z*-mixtures of compound **4c**: (a) thermally in DMSO-d_6 at 100 °C; (b) photochemically in $CDCl_3$ at 25 °C and 360 nm radiation.

Table 2. Spectroscopic Properties of **1c** and **5c**

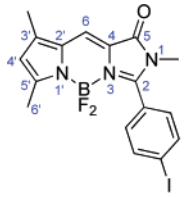

1c

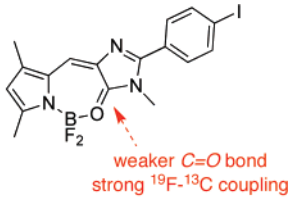

5c

	$\nu_{C=O}$ (cm^{-1})	δ_{C5} (ppm)	δ_{H6} (ppm)	$\delta_{H4'}$ (ppm)	δ_F (ppm)
1c	1705	160.7	7.41	6.01	37.02
5c	1610	158.4 (t, J_{CF} = 6.1 Hz)	7.64	6.28	34.20

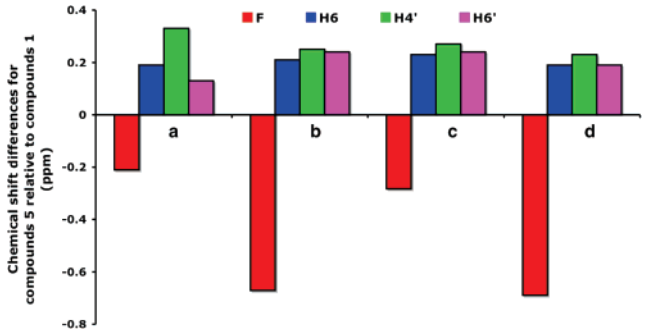

Figure 5. Trends in chemical shift differences for compounds **5** relative to compounds **1** illustrate that these can be used to differentiate between them. Here, the zero line is the chemical shift values for compounds **1**, and the relative chemical shift difference for the corresponding compound **5** is indicated. The chemical shift differences for the ^{19}F signals shown here are 0.1× their actual values.

carbonyl C═*O* only for compounds **5**. Single-crystal X-ray analyses were also obtained for compound **1c** and **5c**, confirming the assignment in this case (see below). Table 2 shows the key spectroscopic parameters for compounds **1c** and **5c**. In retrospect, the magnitude and direction of small chemical shift differences for these two series of compounds show consistent trends (Figure 5) that could be used to make tentative assignments for new compounds in the series.

The X-ray structures of molecules **1c** and **5c** (Figure 6) have at least two interesting features; one is relevant to the spectroscopic assignments made above, and the other relates more to their fluorescence properties. First, the C═O bond length for compound **1c** is 1.226(3) Å, whereas the corresponding distance in compound **5c** is 1.311(5) Å. The first of these carbonyls is not complexed, so the bond length is shorter, and the bond is presumably stronger than in **5c** where its bond order is reduced by interaction with the BF_2 entity. Second, the pyrrole-derived ring in compound **1c** is almost exactly coplanar with the one originating from an imidazolinone; in fact, the dihedral angle between those two rings is only 0.51°. However, for compound **5c** the corresponding dihedral angle is 9.94°. Electronic spectra of compounds **1** and **5** are described in the next section. Briefly, compounds **1** tend to absorb at longer wavelengths than their isomers **5**, with higher extinction coefficients, and they also fluoresce at longer wavelengths. All these properties are consistent with **1** being the more planar, conjugated structure. Moreover, fluorescence quantum yields for **5** are, without

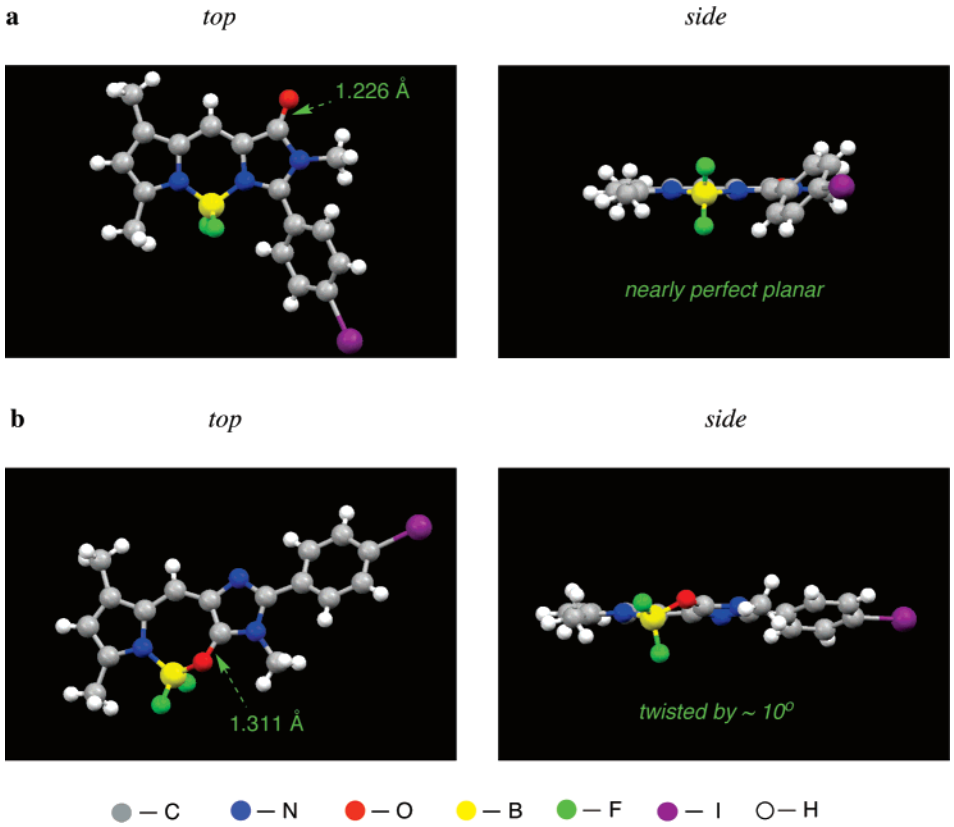

Figure 6. Top and side views of structures based on single molecule X-ray diffraction analyses of (a) compound **1c** and (b) compound **5c**.

exception, 10−100 times less than for the corresponding structures **1**. It may be that one contributing factor to this is rapid equilibration between the two enantiomeric twisted conformations serving as a pathway for radiationless decay.

In the event, *E*,*Z*-isomerization of compounds **4** apparently does not significantly impact the syntheses of products **1** because the isomers seem to interconvert under the conditions used in the final step, as supported by the following observations. Synthesis of **4c** via condensation mediated by HBr/TFA (condition ii in Scheme 1b) in fact gave *E*-**4c** almost exclusively. However, when this material was converted to the boron-containing final products, compound **5c** and **1c** were formed in a ratio of approximately 2:1. Similarly, when a 1:1 mixture of *E*-**4c** and *Z*-**4c** was converted to the boron-containing products via the same reaction conditions, **5c** and **1c** were formed in a ratio of approximately 2:1. It appears that formation of compound **1c** from **4c** is a stereorandom process; i.e., little or no stereochemical information in the starting material is retained.

The pathway outlined in Scheme 1b worked well for syntheses of compounds **1a**−**e**, but there was a problem when the same protocol was applied to the 4-nitrobenzene-substituted product **1f**. Specifically, the intramolecular "aza-Wittig" closure did not afford the desired azlactone **3f**; instead, a complex mixture of products formed. Consequently, the route described in Scheme 2 was devised. Here, the azlactone was formed via an intramolecular condensation of the hippuric acid derivative;[15] this intermediate was not isolated but instead was condensed with 3,5-dimethyl-2-pyrrolaldehyde to give the azlactone derivative **6**. Conversion of **6** to the corresponding imidazolinone **4f** was achieved via reaction with methylamine.[9] Finally, the BF_2 entity was introduced using the same conditions as outlined for the other compounds in the series in Scheme 1b.

Compounds **1f** and **5f** were crystallized and studied by X-ray diffraction. They show the same features as outlined for the structures of **1c** and **5c**. Thus, the carbonyl of **1f** is shorter than that in **5f**, and the molecular shape is almost perfectly flat whereas **5f** is twisted. Further details are given in the Supporting Information.

For synthetic convenience in preparing compounds **1**, concurrent formation of compounds **5** is a nuisance. Conditions to form compounds **1** with high selectivities were not identified in this study, but it was shown that the less fluorescent material **5** could be stripped of the BF_2 group, giving intermediates **4** that could thereby be "recycled" (Scheme 3). Thus, for our most studied compounds, those in series **c**, treatment of **5c** with sulfuric acid gave removal of the BF_2 group to regenerate intermediate **4c**. If this intermediate is not heated above room temperature or radiated with relatively intense and energetic light (e.g., 360 nm), then **4c** will be isolated as a pure *E*-isomer. However, as outlined above, this has no real consequence on the formation of compound **1c** because **5c** is invariably also formed.

Review of the literature on BODIPY dyes leads to the conclusion that there are an abundance of lypophilic probes of that general type but relatively few water-soluble ones.[14] Consequently, there was a strong motivation to prepare the first water-soluble variants of dyes **1**. Compound **1c** was chosen as a starting point because this material was conveniently obtained in gram amounts and because it contains an aryl iodide functionality that can also be manipulated. Sulfonation of compound **1c** was achieved by treatment with excess chlorosulfonic acid at 0 °C (Scheme 4). Practically, isolation of such sulfonic acids can be difficult. Here, the crude reaction mixture was quenched with $NaHCO_{3(aq)}$ and the dye accumulated in the aqueous phase. The dichloromethane layer was removed, and

Scheme 2. Revised Procedure for Synthesis of Compounds **1f** and **5f**

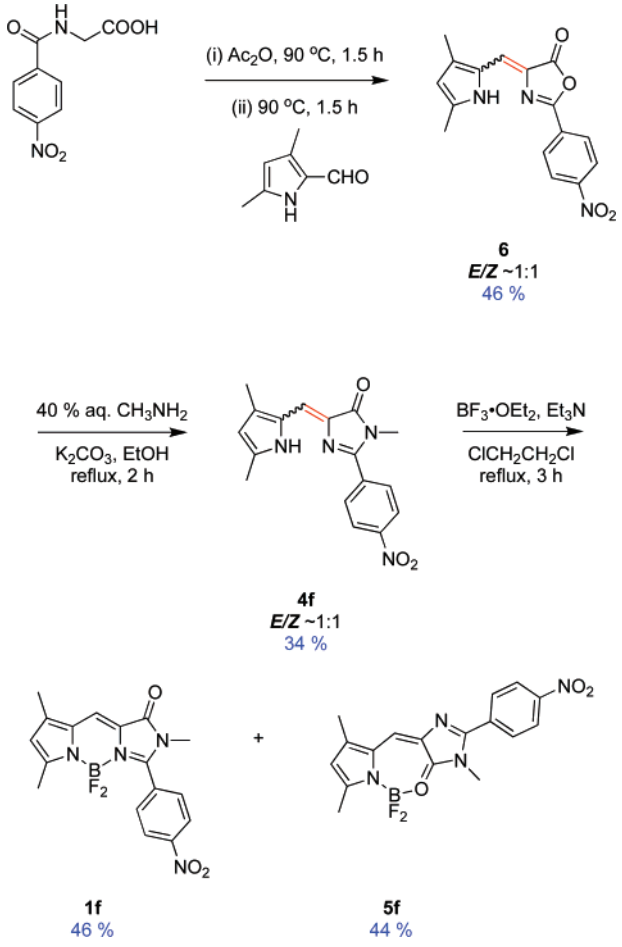

Scheme 3. Method To Recycle the Undesired Compounds **5** into the Target Materials **1**

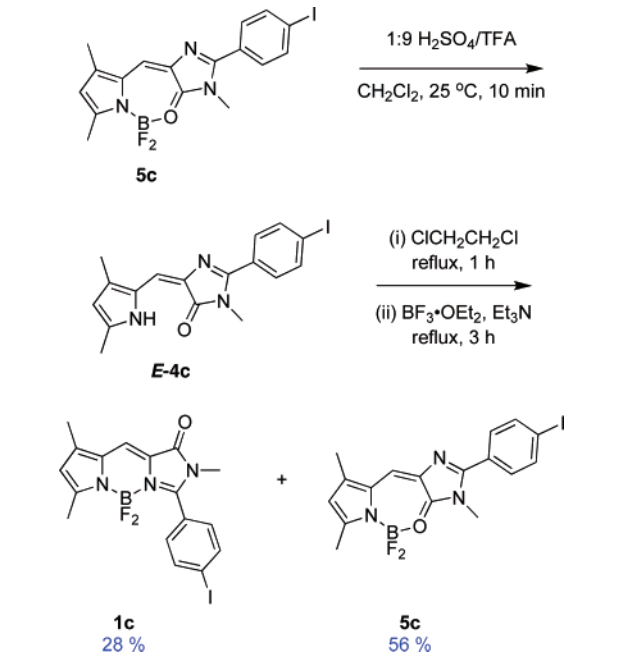

the sodium salt of the product was extracted back into an organic medium (1:1 CH_2Cl_2/^{i}PrOH). After removal of the solvents, the crude residue contained over 90% of the desired product. This material was then further purified by flash column chromatography on silica using 10% MeOH in CH_2Cl_2. Overall, the extraction and chromatography procedures are relatively easy because the products are so strongly colored.

Scheme 4. Syntheses of the Water-Soluble Probes **1g** and **1h**

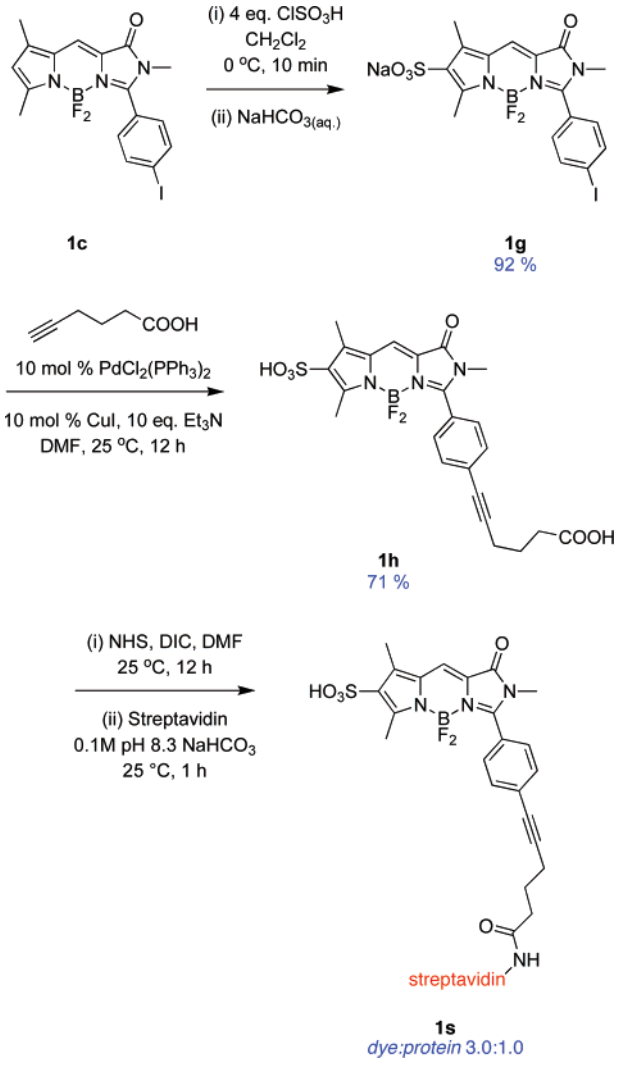

Scheme 4 also shows how the sulfonated product **1g** was coupled with 5-hexynoic acid via a Sonogashira reaction.[22] Again, the sulfonated product could be isolated via column chromatography on silica (20% MeOH in CH_2Cl_2). Compounds **1g** and **1h** are soluble in aqueous media, and **1h** contains a carboxylic acid functionality that could be used as a point of attachment to biomolecules. To illustrate this and to measure the spectroscopic properties of this probe on a protein (see below), **1h** was coupled to streptavidin. Measurement of the dye/protein ratio via UV[23,24] indicated this was almost exactly 3.0:1.0.

UV and Fluorescence Properties of the GFP-Chromophore Analogues. The central hypothesis of this work is that the fluorescence quantum yields of "unconstrained" GFP

(22) Sonogashira, K.; Tohda, Y.; Hagihara, N. *Tetrahedron Lett.* **1975**, *16*, 4467−4470.
(23) *Molecular Probes*; Invitrogen Corporation: Carlsbad, CA, 2006. http://probes.invitrogen.com.
(24) Albarran, B.; To, R.; Stayton, P. S. *Protein Eng.* **2005**, *18*, 147−152.
(25) Weber, G.; Teale, F. W. J. *Trans. Faraday Soc.* **1958**, *54*, 640−648.

Table 3. Spectroscopic Properties of **4c**, **1c**, and **5c** in MeOH

	$\lambda_{max\ abs}$ (nm)	ϵ ($M^{-1}\,cm^{-1}$)	$\lambda_{max\ emiss}$ (nm)	fwhm[a] (nm)	Φ[b]
Z-**4c**	458	40 200	515	69	0.0005
1c	492	57 300	532	54	0.86 ± 0.02
E-**4c**	458	48 000	515	73	0.0003
5c	463	42 700	530	54	0.01

[a] Fluorescence full width at half-maximum peak height (fwhm). [b] Fluorescein in 0.1 M NaOH as standard (ϕ = 0.92).[25]

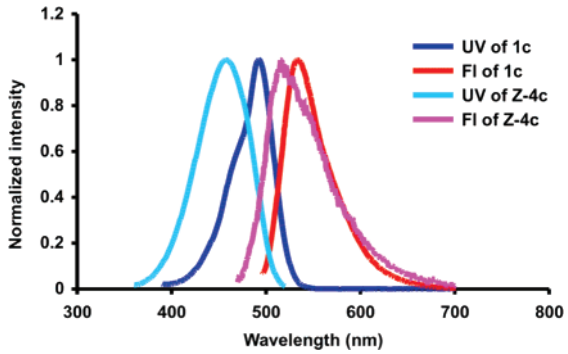

Figure 7. UV absorbance and fluorescence of *Z*-**4c** and **1c** in MeOH (about 10^{-6} M for UV and 10^{-6}–10^{-7} M for fluorescence).

analogues like **4** will be greatly increased in compounds such as **1** that are conformationally locked by a boron atom.

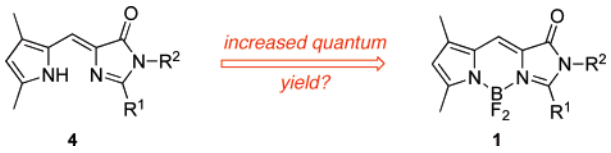

This was verified, and illustrative data are shown in Table 3.

The unconstrained molecule *Z*-**4c** has a very low quantum yield (0.0005) compared to the locked analogue **1c** (0.86); this is a dramatic illustration of the hypothesized effect. Several other differences in the electronic spectra of these materials were also observed. The UV absorbance and fluorescence emissions of compound **1c** are both red-shifted relative to *Z*-**4c**, and the fluorescent emission from **1c** is sharper (Figure 7). For further comparisons, data for the trans-unconstrained intermediate *E*-**4c**, and the isomeric locked product **5c** are also given in Table 3. The UV and fluorescence properties of *E*-**4c** are almost identical to those of *Z*-**4c**. The locked compound **5c** has a quantum yield that is approximately 30-fold greater than *E*-**4c**, and its absorbance and emission wavelengths are also red-shifted. The quantum yield of **5c** is, however, 86-fold less than **1c**, possibly for the reason implied in the discussion of the X-ray structures of **1c** and **5c**, i.e., rapid conformational equilibria between ring-puckered forms leading to radiationless decay pathways. Other consequences of deviation from planarity for **5c** are that the absorbance is blue-shifted and the extinction coefficient is less.

Table 4 gives the UV absorbance and fluorescence data for all the compounds **1** and **5**. The UV and fluorescence properties of the lypophilic compounds **1a**–**f** and **5a**–**f** are quite similar; Figure 8 shows illustrative spectra for compounds **1a**–**f** and **5a**–**f**.

The data in Table 4 show that the UV absorbance maxima for all the lipophilic compounds **1a**–**f** in MeOH are very similar ($\lambda_{max\ abs}$ = 494 ± 4 nm) except for compound **1a**, which has a methyl rather than an aryl substituent on the core. Measurements of fluorescence full width at half-maximum (fwhm) peak heights show that the methyl substituted compound **1a** gives the sharpest fluorescence in the series. Fluorescence emission maxima for compounds **1b**–**e** are in a 10 nm range ($\lambda_{max\ emis}$ = 526 ± 5 nm). The outliers in terms of fluorescence are **1a** (because it does not have an aryl substituent) and the nitroaryl-substituted compound **1f**. Compound **1f**, fluorescing at 598 nm, has a much larger Stoke's shift than the others in the series but a much lower quantum yield. The anomalously low quantum yield is most probably due to photoinduced electron transfer from the excited state of the fluorescent core to the LUMO of the nitroaryl group (i.e., d-PeT). When hexane was used as a medium in place of methanol, then the quantum yield of the nitroaryl-substituted compound **1f** was only about 33% less than **1a**–**e** in MeOH. This implies that the d-PeT quenching mechanism is not dominant in apolar media, reflecting changes of the oxidation potentials in this molecule. The absorption and fluorescence maxima of **1a**–**e** were shifted by up to 20 nm to the red when a less polar media (dichloromethane) was used (see Supporting Information for an expanded version of Table 4).

Table 4. Spectroscopic Properties of GFP-Chromophore Analogues

	$\lambda_{max\ abs}$ (nm)	ϵ ($M^{-1}\,cm^{-1}$)	$\lambda_{max\ emiss}$ (nm)	fwhm (nm)	Φ[a]	solvent
1a	477	57 300	485	19	0.89 ± 0.01	MeOH
5a	426	37 000	485	25	0.0007	MeOH
1b	490	58 700	521	46	0.87 ± 0.01	MeOH
5b	463	50 500	517	64	0.006	MeOH
1c	492	57 300	532	54	0.86 ± 0.02	MeOH
5c	463	42 700	530	54	0.01	MeOH
1d	493	51 300	521	38	0.85 ± 0.03	MeOH
5d	455	38 600	528	69	0.03	MeOH
1e	495	37 900	531	48	0.80 ± 0.01	MeOH
1f	492	44 000	598	120	0.0004	MeOH
1f	498	n.d.	587	53	0.53 ± 0.01	hexanes
5f	473	35 500	527	73	0.005	MeOH
5f	486	n.d.	545	97	0.05	hexanes
1g	488	48 100	531	53	0.88 ± 0.01	MeOH
1g	481	46 500	518	50	0.87 ± 0.01	phos 7.4[b]
1h	488	35 000	538	58	0.84 ± 0.01	MeOH
1h	482	34 800	526	56	0.82 ± 0.01	phos 7.4[b]
1s	482	n.d.	529	56	n.d.	phos 7.4[b]

[a] Fluorescein in 0.1 M NaOH as standard (ϕ = 0.92). [b] 0.1 M lithium phosphate buffer (pH 7.4).

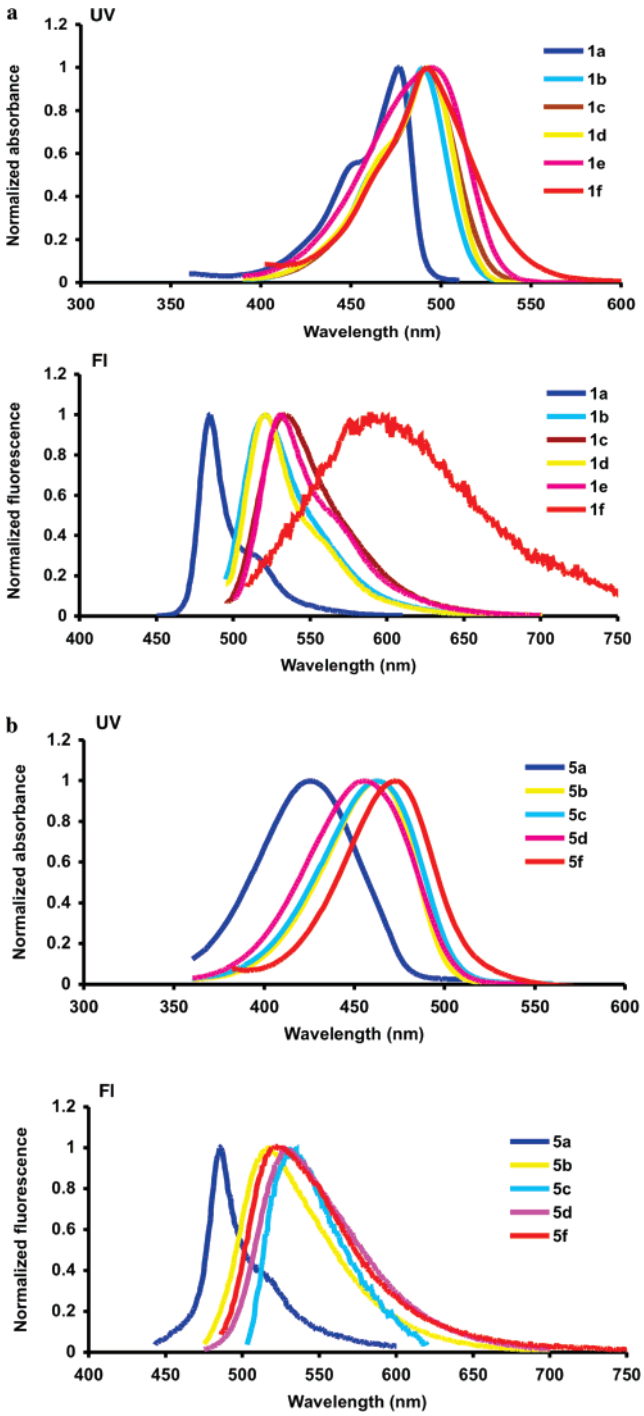

Figure 8. UV absorbance and fluorescence spectra for (a) GFP-chromophore analogues **1** in MeOH and (b) GFP-chromophore analogues **5** in MeOH. Concentrations throughout are 10^{-6} M for UV and 10^{-7} M for fluorescence.

Table 4 also gives data for the water-soluble dyes **1g**, **1h**, and **1s**. The absorbance and emission maxima for **1g** and **1h** were slightly blue-shifted in phosphate buffer relative to the same dyes (and to **1b**−**e**) in MeOH. Quantum yields for **1g** and **1h** were also high in phosphate buffers, just as in MeOH. The spectra of compound **1s**, i.e., **1h** on streptavidin, were not significantly different from that of the parent dye; in other words, conjugation to this particular protein does not have significant effect on the fluorescent properties.

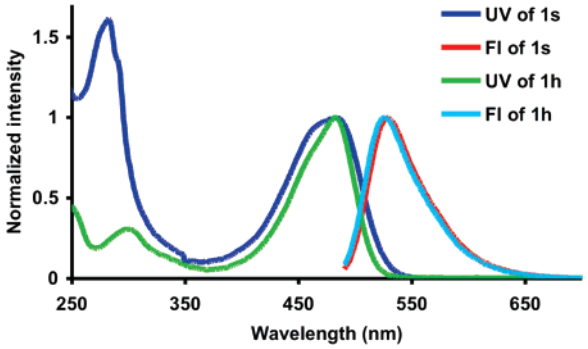

Figure 9. UV absorbance and fluorescence of **1h** and the labeled streptavidin **1s** in 0.1 M lithium phosphate buffer, pH 7.4.

Conclusions

Compounds **1** in this paper are conceptual hybrids of GFP-chromophore analogues and BODIPY dyes. The data presented prove that addition of the BF_2 entities to the open-chain intermediates **4** greatly increases the quantum yields across a range of compounds. Overall, this provides more evidence for the assertion that GFP chromophores within the protein have enhanced quantum yields due to conformational locking within the β-barrel cocoon.

The fluorescence properties of compounds **1** tend to be very similar to those of BODIPY dyes. Both compounds are neutral, uncharged, highly fluorescent molecules that absorb with high extinction coefficients and emit at around 520−530 nm (unless high conjugating substituents are added). BODIPY dyes have many applications in chemistry and biology. Probes **1** could presumably be used in the same ways, and there may be some advantages to doing this, in terms of intellectual property at the very least. Further, the data presented here show that dyes **1** can be sulfonated and modified to include a point of attachment to biomolecules. The water-soluble modifications to compounds **1** result in retention of their fluorescent properties in aqueous media and when attached to a model protein (streptavidin).

Acknowledgment. Financial support for this work was provided by The National Institutes of Health (Grant GM72041) and by The Robert A. Welch Foundation. TAMU/LBMS-Applications Laboratory headed by Dr. Shane Tichy provided mass spectrometric support, the Laboratory for Molecular Simulation (Dr. Lisa Thompson) supported our molecular simulations work, and the X-ray Diffraction Laboratory (Drs. J. Reibenspies and N. Bhuvanesh) generated the crystallographic data.

Supporting Information Available: Procedures and characterization data for all the new compounds and crystallographic files in CIF format. This material is available free of charge via the Internet at http://pubs.acs.org.

JA710388H